

# Simulating low-velocity impact induced delamination in composites by a quasi-static load model with surface-based cohesive contact

Zhang, J. and Zhang, X.

Author post-print (accepted) deposited in CURVE February 2015

## Original citation & hyperlink:

Zhang, J. and Zhang, X. (2015) Simulating low-velocity impact induced delamination in composites by a quasi-static load model with surface-based cohesive contact. Composite Structures, volume 125 : 51–57.

<http://dx.doi.org/10.1016/j.compstruct.2015.01.050>

**Publisher statement:** NOTICE: this is the author's version of a work that was accepted for publication in Composite Structures. Changes resulting from the publishing process, such as peer review, editing, corrections, structural formatting, and other quality control mechanisms may not be reflected in this document. Changes may have been made to this work since it was submitted for publication. A definitive version was subsequently published in Composite Structures [Vol 125 (2015)] Doi: 10.1016/j.compstruct.2015.01.050 .

**Copyright © and Moral Rights are retained by the author(s) and/ or other copyright owners. A copy can be downloaded for personal non-commercial research or study, without prior permission or charge. This item cannot be reproduced or quoted extensively from without first obtaining permission in writing from the copyright holder(s). The content must not be changed in any way or sold commercially in any format or medium without the formal permission of the copyright holders.**

This document is the author's post-print version, incorporating any revisions agreed during the peer-review process. Some differences between the published version and this version may remain and you are advised to consult the published version if you wish to cite from it.

**CURVE is the Institutional Repository for Coventry University**

<http://curve.coventry.ac.uk/open>

## Simulating low-velocity impact induced delamination in composites by a quasi-static load model with surface-based cohesive contact

Jikui Zhang<sup>a</sup>, Xiang Zhang<sup>\*b, c</sup>

<sup>a</sup> Department of Aircraft Design, Beihang University, Beijing 100191, PR China

<sup>b</sup> Aerospace Engineering Division, Cranfield University, Bedford MK43 0AL, UK

<sup>c</sup> Now at: Faculty of Engineering and Computing, Coventry University, Coventry CV1 5FB, UK

### Abstract

In this paper, a computationally efficient finite element model is presented for predicting low-velocity impact damage in laminated composites using a quasi-static load model with surface-based cohesive contact. The effect of compressive through-thickness stress on delamination is taken into account by introducing contact friction force in the shear force direction. Damage onset and propagation in a cross-ply plate  $[90_3/0_3]_S$  is simulated and the numerical results agree well with the experimental observations in terms of damage location, shape and size. Through-thickness stress analysis shows that resistance to the upper interface delamination propagation is mainly contributed by the friction force due to the high compressive through-thickness stress, whereas, for the lower interface, it is the cohesive behaviour that controls the delamination initiation and propagation. Predicted delamination area is not sensitive to the interlaminar friction coefficient when it is greater than 0.6. The range of friction coefficient of the interlaminar contact is recommended to be between 0.6 and 0.9.

**Keywords:** Low-velocity impact; Delamination; Finite element analysis; Surface-based cohesive contact; Friction coefficient

### 1. Introduction

Advanced carbon fiber reinforced plastic (CFRP) has been widely used in the airframe primary structures due to their excellent mechanical properties and low specific weight. However the poor properties in the through-thickness direction make CFRP particularly susceptible to the low velocity impact. Composite laminates exhibit a relatively brittle behaviour and can undergo internal damage in the form of resin crack, fiber fracture and delamination when they are subjected to foreign object impacts. Internal delamination is probably the most critical failure mechanism since they may dramatically reduce the compression strength even when the damage is undetectable by visual inspection from the impact side. Delamination may propagate undetected during the service leading unexpected failure of the component, especially for the primary structures loaded in compression. Therefore, it is essential to develop a computer-based design tool to predict the damage onset and evolution in composite structures under impact.

Different approaches have been reported in the open literature for predicting the delamination initiation and propagation in impacted laminates. They can be broadly divided into three categories: strength-based failure models [1-4], fracture mechanics based models using either the virtual crack

---

\* Corresponding author

Tel.: +44 2477658599; E-mail: [xiang.zhang@coventry.ac.uk](mailto:xiang.zhang@coventry.ac.uk) (X. Zhang); [zjk@buaa.edu.cn](mailto:zjk@buaa.edu.cn) (J. Zhang)

closure technique (VCCT) [5-6] or cohesive zone models (using either cohesive [7-9] or spring [10] elements at the interface), and the continuum damage mechanics (CDM) approaches [11-14]. Among them, the cohesive zone models, which combine the strength-based failure criteria with fracture mechanics energy criteria, have attracted considerable interests in recently years and been used for simulation of discrete damage and failure [15], since they allow overcoming the main limitations of the VCCT approach.

Although many cohesive zone models have achieved acceptable prediction e.g. [10, 15], two technical issues have affected the computational accuracy and efficiency.

First, pre-determined interfaces (where delamination may occur) are currently modelled by either the cohesive [7-9] or spring elements [10]. Both are computationally demanding. The cohesive interface elements are expected to be several times smaller than the surrounding elements (often in fine mesh) to ensure numerical convergence. The spring elements also have the potential problems of local stress concentration. It is not yet possible to use these finite element models as a design tool even for simple plates, let alone realistic structures.

Second, most research [15, 16] simulates the delamination initiation by using the stress-based quadratic failure criterion and subsequent propagation by a linear softening model. The result is reasonable when the interface is subjected to tension stress in the through-thickness direction. However, serious difficulty arises when dealing with delamination induced by impact loading due to high compressive stress, which could improve the laminate interlaminar shear strength considerably. Hou et al. [17] firstly suggested that delamination is totally constrained by compressive through-thickness stress and therefore a smaller damage was predicted. Subsequently, an empirical delamination criterion was developed by Hou et al. [18], which allow delamination to initiate and propagate under high interlaminar shear stress when the out-of-plane compression is relatively low. To take account of compression, Li et al. [19] modified the failure initiation and propagation criteria by using a pre-determined parameter to relate the compression with the increase in interlaminar shear strength and the mode II critical fracture energy. Zhang et al. [20] treated the influence of the compressive through-thickness stress by adding the contact-induced friction between the adjacent plies. The friction stress at the interface can inhibit the delamination initiation and propagation. However, the model is time-consuming due to multiple contact interfaces and use of very fine cohesive elements.

The aim of this paper is to develop a more efficient design tool for predicting the low velocity impact damage. A surface-based cohesive contact model is employed to take account of the effect of out-of-plane compressive stress on the delamination onset and propagation. It is aimed to reduce the computation time comparing with the friction contact model previously developed [20] since there are no cohesive interface elements in the current model. To further increase the computational efficiency, quasi-static loading was applied in the model to simulate the dynamic impact loading as the CFRP laminates exhibit similar contact force and damage magnitudes under the transverse low velocity impact and quasi-static loading [21-24].

## **2. Description of surface-based cohesive contact approach**

Cohesive interface element model has been employed by many researchers to simulate the delamination growth in composite laminates. The failure of cohesive element is based on the interactive mixed mode criteria for both the initiation and propagation of the delamination. The

model works very well if the through-thickness normal stress is in tension, which can also be accounted for in combination with the interlaminar shear stresses. However, when the through-thickness stress is compressive, its effect on delamination suppression is usually ignored and the failure of interface is considered to be pure mode II [19]. However, the compressive through-thickness stress induced by low-velocity impact is considerable high that greatly increases the interlaminar shear strength, especially for the upper interface close to the impact point. In this paper, a surface-based cohesive contact model based on the ABAQUS commercial software is developed to consider the effect of compressive through-thickness stress.

Surface-based cohesive contact [25] allows the specification of generalised traction-separation behaviour for two adjacent surfaces. This behaviour offers capabilities of modelling failure that are very similar to the cohesive element that are defined using a traction-separation law. However, this surface-based cohesive behaviour is typically easier to define and allows simulation of a wider range of cohesive interactions, such as the interlaminar delamination and contact phenomena of composite laminate subjected to impact load. The internal load transfer behaviour of surface-based cohesive contact is illustrated in Fig. 1.

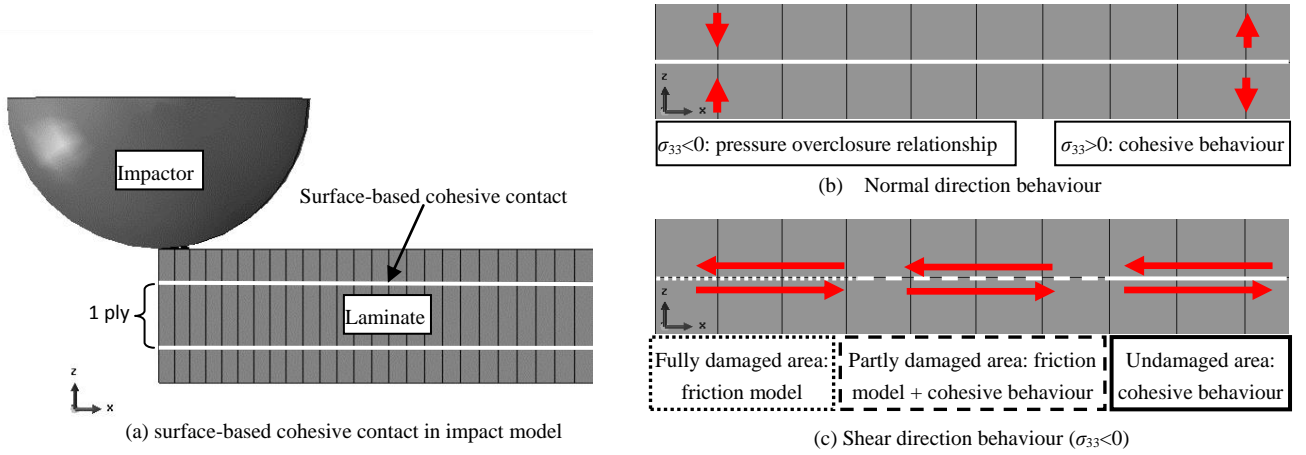


Fig. 1 Schematic of load transfer behaviour of surface-based cohesive contact model

In the contact normal direction, the compressive behaviour between the contacted surfaces was governed by the so-called pressure overclosure relationship. In contrast, the cohesive behaviour contributes to the contact normal stress ( $\sigma_{33}$ ) when the interface is subjected to tensile stress in the through-thickness direction, as shown in Fig. 1b.

In the shear direction, the 'net' shear force is a combination of the cohesive action and the contribution from the friction force. The load distribution depends on the damage extent of the cohesive interface, as shown in Fig. 1c. If the cohesive stiffness is un-degraded, it is assumed that the cohesive model is active and the friction model is dormant. Once the cohesive stiffness starts degrading, the cohesive contribution to the shear stresses starts decreasing with the damage evolution. Consequently, the friction model activates and begins contributing to the shear stresses. The elastic stiffness of the friction model is ramped up in proportion to the degradation of the elastic cohesive stiffness. Once the maximum degradation has been reached, the cohesive contribution to the shear stresses is zero, and the only contribution to the shear stresses is from the friction force.

For the cohesive behaviour of contact surface, damage onset is modelled by a strength-based criterion, whereas damage propagation is predicted by a fracture mechanics criterion. Details are given in Section 3.

### 3. Finite element model

A published low velocity impact test [26] was modelled. Test specimen of  $87.5 \times 65$  mm in size was fabricated from Seal HS160/REM unidirectional carbon/epoxy prepreg with stacking sequence  $[90_3/0_3]_s$  resulting in 2 mm nominal thickness. The specimen was simply supported in test by a steel plate with a rectangular cutout of  $67.5 \times 45$  mm underneath the specimen. The diameter of the hemispherical impactor was 12.5 mm.

The rectangular test specimen was modelled by using the commercial software package ABAQUS. Only one quarter of the specimen was modelled due to the geometric symmetry, as shown in Fig. 2a. The four cutout edges of the specimen are constrained by the simply supported boundary condition. The laminate is modelled by continuum solid element (designated as C3D8 in ABAQUS) with assembled mechanical properties from the ply properties as given in Table 1, where  $E_{11}$ ,  $E_{22}$  and  $E_{33}$  are the Young's modulus in the fiber, transverse and normal direction respectively,  $G_{12}$ ,  $G_{13}$  and  $G_{23}$  are the shear modulus,  $\nu_{12}$ ,  $\nu_{13}$  and  $\nu_{23}$  are the Poisson's ratio,  $Y_T$  is the matrix tension strength,  $S_{xy}$  and  $S_{yz}$  are the shear strength. The smallest element size in the impact zone is  $0.23 \times 0.27$  mm. Each elements layer represents one lamina ply in the model. A total number of 100,980 nodes and 79,968 solid elements are used to model the impacted laminate. The impactor was modelled as a rigid body indenter due to the relatively smaller deformation of the impactor compared with the laminate. The interaction between the plate and the indenter was simulated by surface-to-surface contact pairs. A friction model was included in the contact property definition and a friction coefficient of 0.3 is selected.

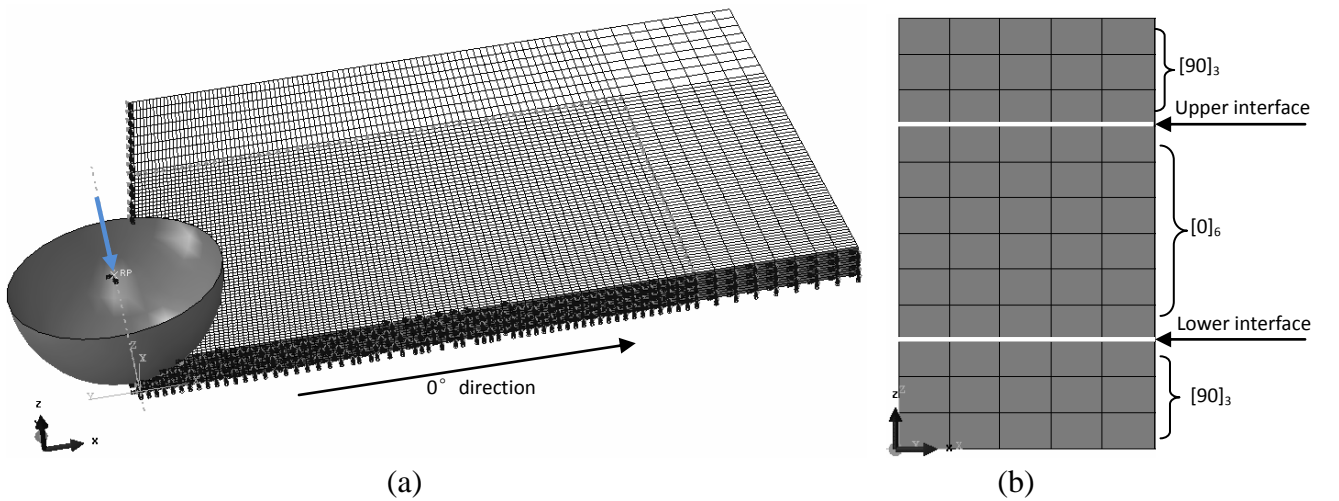


Fig. 2 (a) FE model and (b) definition of surface-based cohesive contact

Table 1. Materials properties of HS160/REM laminate [26]

Lamina ply	Cohesive interface
Elastic modulus (GPa)	Stiffness (GPa/m)
$E_{11}=93.7, E_{22}=E_{33}=7.45, G_{12}=G_{13}=G_{23}=3.97$	$K_N=120000, K_S=K_T=43000$
Poisson's ratio $\nu_{12}=\nu_{13}=\nu_{23}=0.261$	Strength (MPa) $N=30, S=T=80$
Matrix tension and shear strength (MPa)	Critical strain energy release rate (J/m <sup>2</sup> )
$Y_T=30 \quad S_{xy}=S_{yz}=80$	$G_{IC}=520 \quad G_{IIC}=G_{IIIC}=970$

Hashin's matrix failure criterion and stiffness degradation model are adopted to simulate the matrix cracking, as given in Table 2, where  $E_{22,d}$ ,  $G_{xy,d}$  and  $G_{yz,d}$  are the degraded transverse and shear modulus. A user defined subroutine (designated as USDFLD in ABAQUS) are developed for implementation of the Hashin matrix failure criterion. Since no delamination was expected between the plies of the same fiber orientation, surface-based cohesive contact were only inserted between the plies having different fiber orientations. For the stacking sequence  $[90_3/0_6/90_3]$ , two interfaces shown in Fig. 2b are defined by the surface-based cohesive contact, i.e. the upper interface 90/0 and lower interface 0/90. The elastic properties and fracture parameters of interface used in the model are given in Table 1, where  $t_n$ ,  $t_s$ ,  $t_t$  are the interface stresses in the normal and two shear directions,  $N$ ,  $S$ ,  $T$  are the interface strength under the mode I, II and III respectively. Failure criteria of interface used in this work are given in Table 2, where  $G_I$ ,  $G_{II}$ ,  $G_{III}$  represent the strain energy release rate and  $G_{IC}$ ,  $G_{IIC}$ ,  $G_{IIIC}$  are the critical strain energy release rate under the mode I, II and III respectively. The failure criterion of interface is implemented in the ABAQUS code without the need of defining any special elements or user specific code.

Table 2. Failure criteria of interface used in this work

Damage form	Damage initiation	Damage propagation
	Hashin's criterion	Material property degradation
In-plane matrix cracking [27]	$\left(\frac{\sigma_{yy}}{Y_T}\right)^2 + \left(\frac{\sigma_{xy}}{S_{xy}}\right)^2 + \left(\frac{\sigma_{yz}}{S_{yz}}\right)^2 = 1$	$E_{22,d} = 0.2E_{22} \quad G_{xy,d} = 0.2G_{xy} \quad G_{yz,d} = 0.2G_{yz}$
Cohesive contact interface[26]	Stress-based quadratic criterion $\left(\frac{t_n}{N}\right)^2 + \left(\frac{t_s}{S}\right)^2 + \left(\frac{t_t}{T}\right)^2 = 1$	Mix-mode power lower $\left(\frac{G_I}{G_{IC}}\right) + \left(\frac{G_{II}}{G_{IIC}}\right) + \left(\frac{G_{III}}{G_{IIIC}}\right) = 1$

To save the computation time, quasi-static load is applied to simulate the low-velocity impact in this paper. The displacement in the Z-direction instead of velocity is applied to the impactor. The similarity of quasi-static load and low-velocity impact in terms of the contact force and damage areas has been reported by various researchers [21-24], which demonstrate that the relation between the impact force and displacement is not changed by the impact velocity in the low velocity range. This is because that the influence of inertia caused by the dynamic load is very small and thus can be neglected. However, it is should be noted that the quasi-static load model cannot provide the contact force versus time history. Moreover, the applicability of quasi-static load assumption needs to be checked carefully if the impact velocity is above the low-velocity range.

In this study, ABAQUS/Standard code was used for the quasi-static load model. The analyses were carried out on a Linux cluster workstation with an Intel E5-2660 CPU having a total of 8 CPU cores. It takes just under 2 h (1 h and 52 min) for a typical simulation run. Table 3 shows a comparison of the FE models used in this study and previously developed by the same research group [20], treating the influence of compressive through-thickness stress by adding the contact-induced friction between the adjacent plies. Both models delivered acceptable results in terms of the delamination shape and size. Since there are no cohesive interface elements implemented in the model of this study, the computational time is reduced considerably comparing to the contact model in [20], which took about 8 h using the same computing facility.

Table 3. FE model comparison of presented by this study and previously developed [20]

FE Model	This study	Previously developed [20]
Modelling compressive through-thickness stress effects	Surface-based cohesive contact	Cohesive interface elements & contact
Crack modelling approach	Hashin's criterion	Cohesive failure behaviour
Load assumption	Quasi-static load assumption	
Computational time	1 hour and 52 minutes	About 8 hours

## 4. Result and discussion

### 4.1 Experimental validation

Numerical simulation of the impact behaviour and damage size of the  $[90_3/0_3]_s$  laminates and comparison with experimental result are reported by [26]. For the impact energy ( $E$ ) of 1.5 J, the maximum deflection in the Z-direction is 1.8 mm. This displacement is applied to the impactor under the displacement-control loading in the quasi-static load model. The friction coefficient of 0.6 is selected for modelling the interlaminar friction.

Fig. 3 shows the predicted impactor contact force versus applied displacement by the quasi-static load model. The slope of the predicted curve is slightly lower than the experimental curve [26]. This can be explained that the inertial force of the composite laminates is neglected in the quasi-static load model, which could absorb some impact energy during the loading period.

It is worth noting that the slope of the force versus displacement curve changes at point A, when the impactor force equals to 1200 N approximately. This change of the slope of the curve indicates the reduction of laminate stiffness due to the onset of the delamination and is captured by the quasi-static load model accurately. The damage sizes of the interfaces at point A are shown in Fig. 4. The delamination onset occurred in both the upper and lower interfaces. However the delamination on the upper interface is inhibited by the high compressive through-thickness stresses due to the contact between impactor and laminate.

Predicted damage area and comparison with a reference model and test measurement [26] are shown in Fig. 5. Reasonably good agreement is achieved by this model in terms of damage width and length. The modelling result shows that the quasi-static load model with surface-based cohesive contact is capable of simulating the composite laminate delamination onset and propagation caused by low-velocity impact.



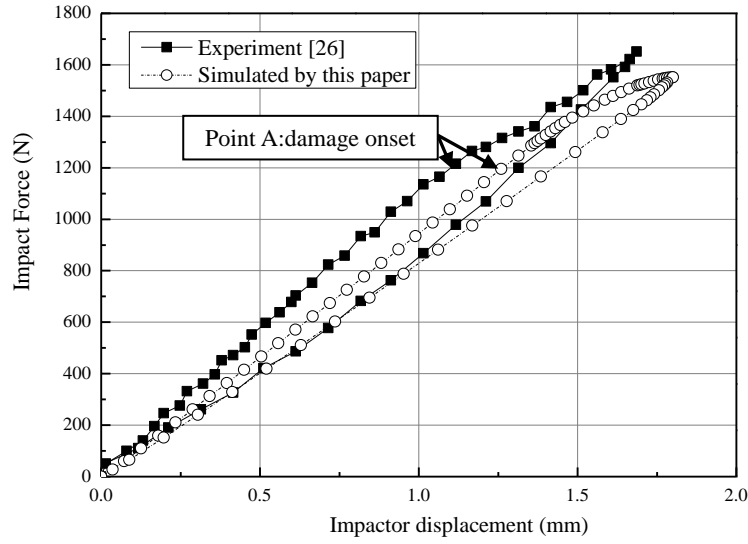


Fig. 3 Relationship of impactor contact force versus displacement ( $\mu=0.6$ ;  $E=1.5$  J)

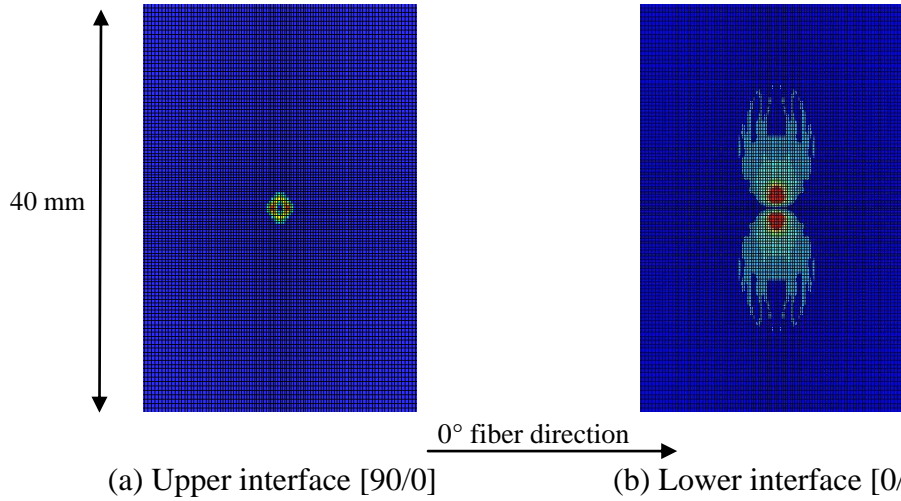


Fig. 4 Predicted damage size at point A of load~displacement curve ( $\mu=0.6$ ;  $E=1.5$  J)

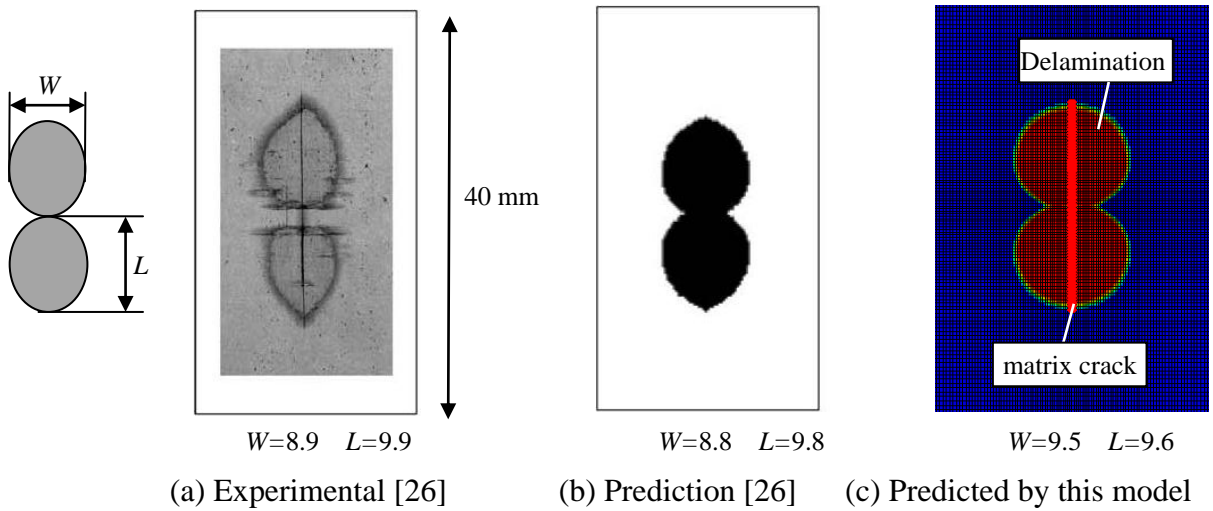


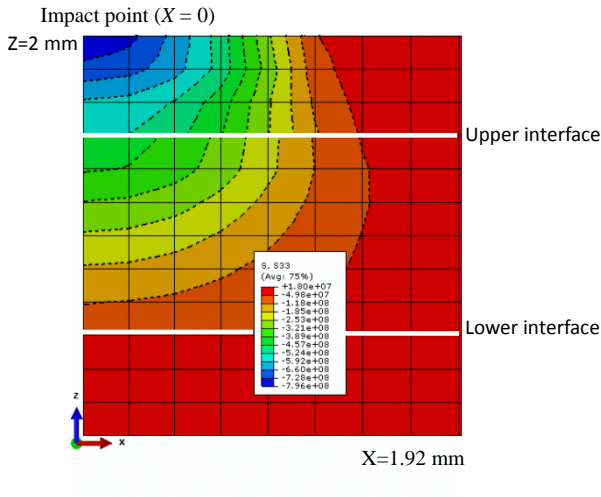
Fig. 5 Comparison delamination at lower interface of numerical prediction and experimental measurement (unit: mm,  $\mu=0.6$ ;  $E=1.5$  J)



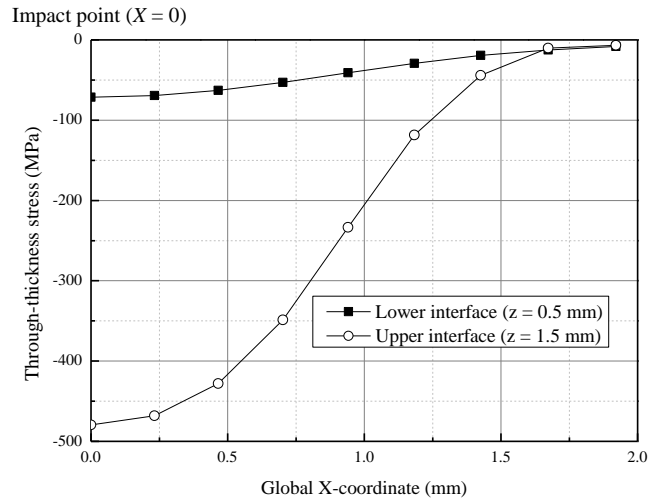
#### 4.2 Compressive through-thickness stress distribution and influence

It is known that the out-of-plane compressive stress can apparently improve the interlaminar shear strength by suppressing delamination initiation and propagation. However, the choice of an appropriate criterion for prediction of delamination under compressive loading is still a subject of further research. Representative models are reported in [18-19], including the strengthening effect of through-thickness compression on the shear strength. In this paper, the surface-based cohesive contact model available in ABAQUS software is defined to describe the cohesive and contact behaviour of the interface during impact process. The effect of the through-thickness compression is taken into account by the calculated contact friction force.

Calculated through-thickness stresses distribution at the applied displacement of 1.8 mm is shown in Fig. 6. Stress concentration is high in the area adjacent to the impact point and rapidly decreased along both the X and Z directions. The compressive through-thickness stress is much higher at the upper interface than the lower interface, as shown in Fig. 6b. The interlaminar delamination propagation of the upper interface is inhibited by the high shear force at the centre of the laminate (shown in Fig. 7a), which is mainly contributed by the contact induced friction force due to the high compressive through-thickness stress.

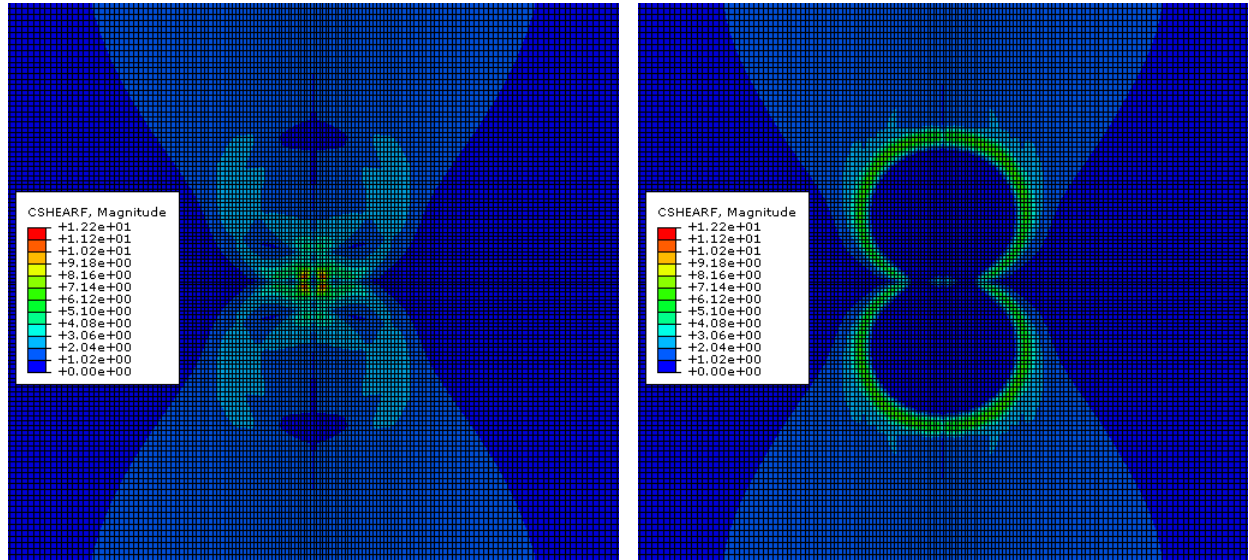


(a) Stress contour (unit: Pa)



(b)  $\sigma_{33}$  versus X-coordinate

Fig. 6 Distribution of through-thickness normal stress ( $\sigma_{33}$ )



(a) Upper interface [90/0]

(b) Lower interface [0/90]

Fig. 7 Distribution of shear force on the contact surface (unit: N)

In the lower surface, the contact induced friction force arising from the compressive through-thickness stress is much lower (Fig. 6b) and not sufficient to restrain the interlaminar delamination onset and propagation. The contact surface shear force is much higher at the border of the delamination area that is far away from the impact point (Fig. 7b) and compressive through-thickness stress is very low (Fig. 6b). This indicates the resistance to delamination propagation is mainly contributed by the interface cohesive failure behaviour.

It should be pointed out that surface-based cohesive contact has two advantages comparing with the reported models [18-20] in dealing with the effect of the compressive through-thickness stress.

First, both models in [18, 19] take the effect of through-thickness compression by revising the delamination initiation and propagation criterion. A specific and potentially complicated user defined subroutine ('VUMAT' or 'UMAT' in ABAQUS) needs to be developed for implementation of the cohesive behaviour of interface elements due to this revision. The friction model in [20] takes a significant amount of computing time. Surface-based cohesive contact model used in this model adopts the delamination initiation and propagation criterion offered by ABAQUS software and the effect of the through-thickness compression is taken into account by the contact friction force directly. Therefore, it is easier to use compared to the models developed reported in [18-20].

Second, the surface-based cohesive contact model in this paper is different from the cohesive zone model [7, 15] in terms of the modelling approach to the shear behaviour in damaged area. In cohesive zone model [15], failed cohesive elements are not removed from the FE model so as to avoid compenetrations between the delaminated layers. However, the contact friction force is totally ignored that makes no contribution to prevent the damage from propagation. In this paper, the contact friction force in damaged area is taken into account, which can be high enough to retard the damage propagation if the normal contact stress is relatively high enough.

#### 4.3 Influence of interlaminar friction coefficient

The influence of the through-thickness compression to the shear strength is simulated by a

surface-based cohesive contact model with the friction force in the shear direction. The friction force is a function of the contact force as well as the coefficient of friction. Research has shown that for the CFRP, interlaminar friction coefficient ( $\mu$ ) is within the range of 0.6~0.8 [28, 29]. A sensitivity analysis is conducted by selecting different values of friction coefficient (0.5, 0.6, 0.7, 0.8, and 0.9) in the contact model. Predicted delamination areas at the upper and lower interfaces are illustrated in Fig. 8. The following observations can be made.

First,  $\mu = 0.5$  gives considerably different delamination area on both the upper and lower interfaces comparing with all other friction coefficients (0.6, 0.7, 0.8, and 0.9). Much larger delamination area is predicted at the upper interface, indicating that calculated friction force is too small to inhibit the initiation and propagation of interlaminar delamination. It should be noted that the impactor was applied with 1.8mm deflection in the Z-direction under the displacement-controlled model. Delamination of the upper interface results in stiffness degradation of the laminate, which could explain the smaller delamination area predicted at the lower interface.

Second,  $\mu = 0.6, 0.7, 0.8$ , and  $0.9$  gives the similar delamination size and shape on both the upper and lower interfaces. Delamination at the upper interface is initiated at the region adjacent to the impact point where the shear stress is relative high. However, it was inhibited to grow further by the friction force caused by the high compressive through-thickness stress. At the lower surface, interlaminar delamination could initiate and propagate since the compressive through-thickness stress is much lower (Fig. 6b). Once the delamination has propagated far away from the impact point, the effect of friction force on the delamination can be ignored as the compressive through-thickness stress is negligibly low (Fig. 6b).

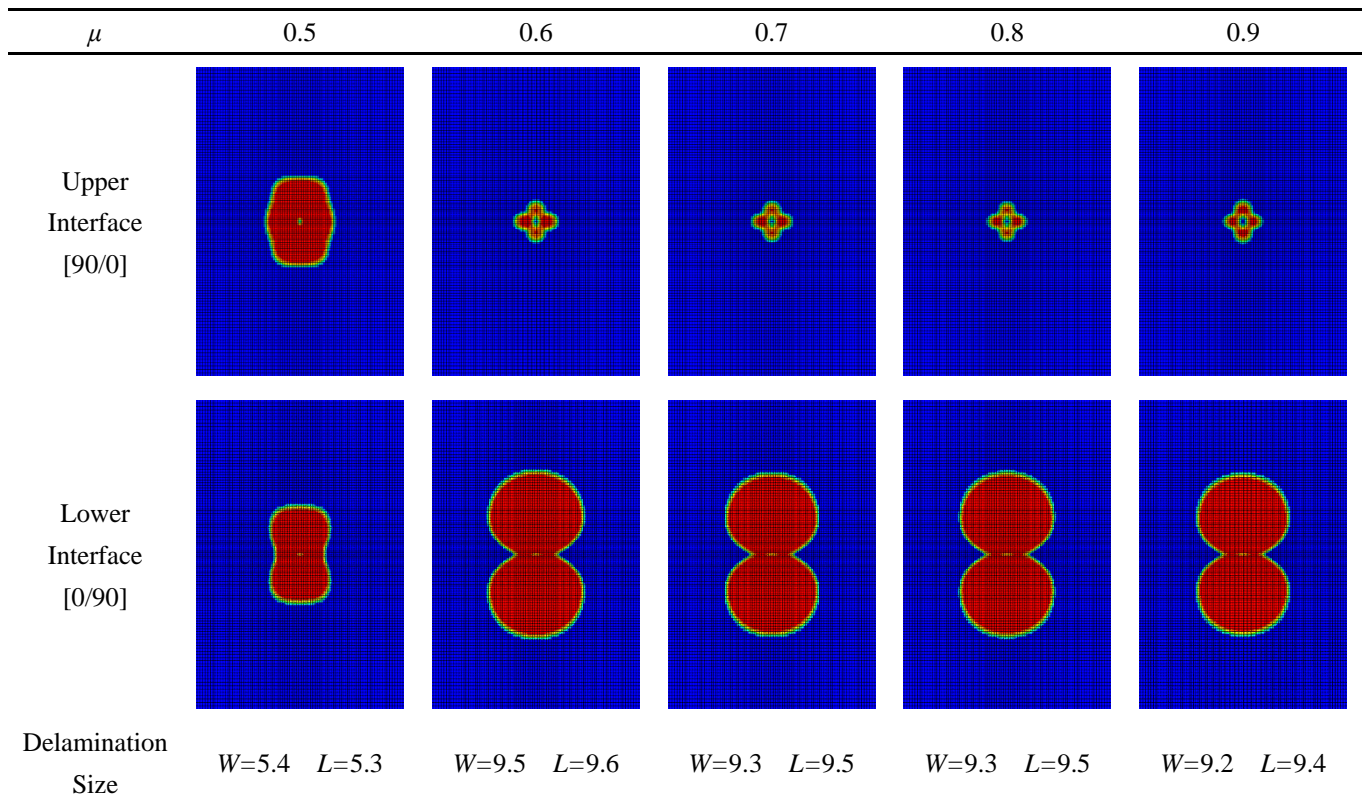


Fig. 8 Influence of interlaminar friction coefficient ( $\mu$ ) on predicted delamination area ( $E=1.5$  J)

To summarise, delamination area is very sensitive to the value of the interlaminar friction coefficient

if it is under 0.6. However, once it is greater than 0.6, delamination at the upper interface is inhibited by the friction force and similar delamination area is predicted for various values within the range of 0.6-0.9. This means that the interlaminar friction coefficient could be selected from 0.6 to 0.9 in similar analysis. This is value broadly comparable with the measured value of  $\mu = 0.8$  [28] and  $\mu = 0.6$  [29] for CFRP materials.

## 5. Conclusions

A computationally efficient model has been developed for predicting the low-velocity impact damage in laminated composites. The two novel features are: (a) using the surface-based cohesive contact model available in the ABAQUS package to avoid using numerous interface cohesive elements, (b) using quasi-static loading in the FE model to simulate the low-velocity impact load. Based on the simulation of a cross-ply laminate, following conclusions can be drawn.

Quasi-static load model in conjunction with surface-based cohesive contact is easy to use and efficient to simulate the shear-driven delamination and ply interactions due to the compressive through-thickness stress.

For a cross-ply laminate  $[90_3/0_3]_S$ , resistance to the upper interface delamination propagation comes mainly from the friction force arising from the high compressive through-thickness stress, whereas, for the lower interface, it is the cohesive behaviour that controls the delamination initiation and propagation.

Predicted delamination area is not sensitive when the interlaminar friction coefficient is greater than 0.6. For carbon fibre epoxy composites, the friction coefficient of the interlaminar contact is recommended to be within the range of 0.6 and 0.9.

**Acknowledgement:** J. Zhang thanks the China Scholarship Council for supporting his visit to Cranfield University where this study was performed.

## Reference

- [1] Choi HY, Chang FK. A model for predicting damage in graphite/epoxy laminated composites resulting from low-velocity point impact. *Journal of Composite Materials*. 1992, 26: 2134-69
- [2] Brewer JC, Lagace PA. Quadratic stress criterion for initiation of delamination. *Journal of Composite Materials*. 1988, 22:1141-55
- [3] Tita V, Carvalho J, Vandepitte D. Failure analysis of low velocity impact on thin composite laminates: Experimental and numerical approaches. *Composite Structures*. 2008, 83:413–28
- [4] Farooq U, Myler P. Efficient computational modelling of carbon fibre reinforced laminated composite panels subjected to low velocity drop-weight impact. *Materials & Design*. 2014, 54: 43-56.
- [5] Fleming DC. Delamination modeling of composites for improved crash analysis. National Aeronautics and Space Administration, Langley Research Center, Hampton, Virginia, USA, 1999, NASA/CR-1999-209725.
- [6] Ronald K. Virtual crack closure technique: History, approach, and applications. *Applied Mechanics Reviews*, 2004, 57:109-43
- [7] Aymerich F, Dore F, Priolo P. Prediction of impact-induced delamination in cross-ply composite laminates using cohesive interface elements. *Composites Science & Technology*. 2008, 68: 2383-90.
- [8] Shi Y, Soutis C. A finite element analysis of impact damage in composite laminates. *The Aeronautical Journal*. 2012, 116:1131-47
- [9] Caputo F, De Luca A, Lamanna G, et al. Numerical study for the structural analysis of composite

laminates subjected to low velocity impact. *Composites: Part B*. 2014,67:296–302

- [10] Bouvet C, Castanié B, Bizeul M, et al. Low velocity impact modelling in laminate composite panels with discrete interface elements. *Int- Journal of Solids and Structures*. 2009, 46: 2809-21
- [11] Donadon MV, Iannucci L, Falzon BG, et al. A progressive failure model for composite laminates subjected to low velocity impact damage. *Computers & Structures*. 2008, 86:1232-52
- [12] Kim EH, Rim MS, Lee I, et al. Composite damage model based on continuum damage mechanics and low velocity impact analysis of composite plates. *Compos Struct* 2013, 95: 123-34
- [13] Riccio A, De Luca A, Di Felice G., et al. Modelling the simulation of impact induced damage onset and evolution in composites. *Composites: Part B*. 2014,66 : 340–47
- [14] Batra RC, Gopinath G, Zheng JQ. Damage and failure in low energy impact of fiber-reinforced polymeric composite laminates. *Composite Structures* 2012,94: 540–47
- [15] Feng D, Aymerich F. Finite element modelling of damage induced by low-velocity impact on composite laminates. *Composite Structures* 2014,108,161–71
- [16] AB de Moraes. Mode I cohesive zone model for delamination in composite beams. *Engineering Fracture Mechanics*. 2013,109:236–45
- [17] Hou JP, Petrinic N, Ruiz C, et al. Prediction of impact damage in composite plates *Composites Science and Technology*. 2000, 60 : 273-81
- [18] Hou JP, Petrinic N, Ruiz C. A delamination criterion for laminated composites under low-velocity impact. *Composites Science and Technology*. 2001,61: 2069–74
- [19] Li XQ, Hallett SR, Wisnom MR. Predicting the effect of through-thickness compressive stress on delamination using interface elements. *Composites: Part A*. 2008,39 :218–30
- [20] Zhang X, Bianchi F, Liu H.Q. Predicting low-velocity impact damage in composites by a quasi-static load model with cohesive interface elements. *The Aeronautical Journal*. 2012,116: 1367-81
- [21] Luo GM, Lee YJ. Quasi-static simulation of constrained layered damped laminated curvature shells subjected to low-velocity impact. *Composites: Part B*. 2011, 42:1233–43
- [22] Sutherland LS, Guedes Soares C. The use of quasi-static testing to obtain the low-velocity impact damage resistance of marine GRP laminates. *Composites: Part B* 2012, 43: 1459–67
- [23] Yokozeki T, Kuroda A, Yoshimura A, et al. Damage characterization in thin-ply composite laminates under out-of-plane transverse loadings. *Composite Structures* 2010, 93: 49–57
- [24] Brindle AR, Zhang X. Predicting the compression-after-impact performance of carbon fibre composites based on impact response. *Proc of 17th Int Conf in Composite Materials (ICCM17)*, Edinburgh, UK, 27-31 July 2009
- [25] Abaqus analysis user's manual 6.11, 35.1.10. Surface-based cohesive behaviour.
- [26] Aymerich F, Dore F, Priolo P. Simulation of multiple delaminations in impacted cross-ply laminates using a finite element model based on cohesive interface elements. *Compos Sci & Tech*. 2009, 69:1699-1709
- [27] Tserpes KI, Labeas G, Papanikos P, et al. Strength prediction of bolted joints in graphite/ epoxy composite laminates. *Composites Part B*. 2002, 33: 521-29
- [28] Wisnom MR, Li DS. Modelling damage initiation and propagation in composites using interface elements. *CADCOMP*, Southampton; 1994.
- [29] Schon J. Coefficient of friction of composite delamination surfaces, *Wear*. 2000, 237:77-89.